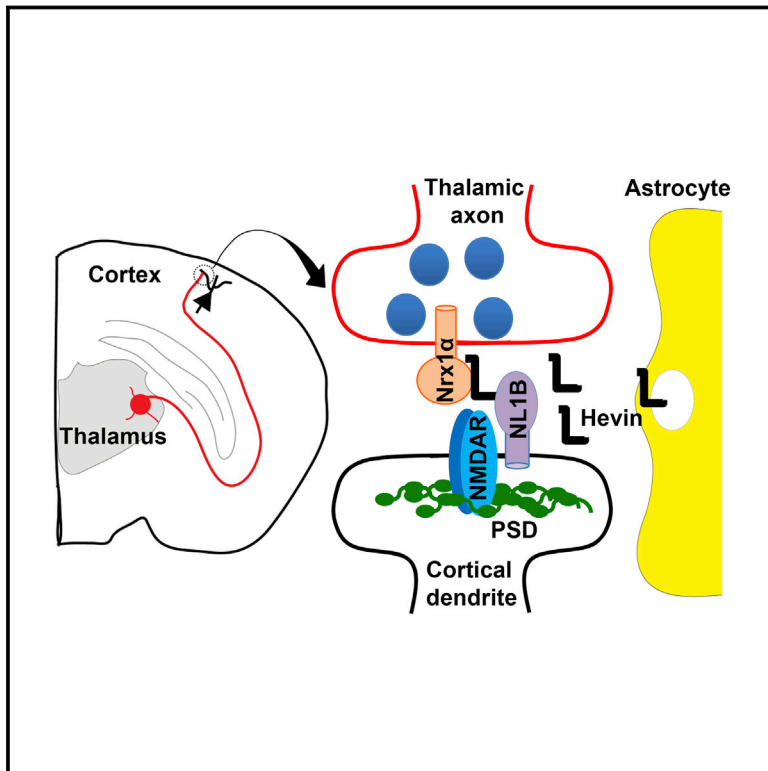


Astrocytes Assemble Thalamocortical Synapses by Bridging NRX1 α and NL1 via Hevin

Graphical Abstract



Authors

Sandeep K. Singh, Jeff A. Stogsdill, Nisha S. Pulimood, ..., Ru-Rong Ji, Alexandre E. Medina, Cagla Eroglu

Correspondence

sandeep.singh@duke.edu (S.K.S.), cagla.eroglu@dm.duke.edu (C.E.)

In Brief

Astrocytes promote synapse formation and plasticity by secreting a protein that bridges non-interacting isoforms of neurexin and neuroligin, suggesting an additional layer of complexity to the isoform code that dictates synaptic adhesion.

Highlights

- Astrocyte-secreted hevin is a pre- and postsynaptic organizer
- Hevin induces thalamocortical synapse formation by bridging NRX1 α and NL1
- Hevin is required for recruitment of NL1 and NMDAR to excitatory synapses *in vivo*
- Astrocyte-secreted hevin is necessary for ocular dominance plasticity



Astrocytes Assemble Thalamocortical Synapses by Bridging NRX1 α and NL1 via Hevin

Sandeep K. Singh,^{1,8,*} Jeff A. Stogsdill,^{1,8} Nisha S. Pulimood,² Hayley Dingsdale,¹ Yong Ho Kim,³ Louis-Jan Pilaz,⁴ Il Hwan Kim,¹ Alex C. Manhaes,² Wandilson S. Rodrigues, Jr.,² Arin Pamukcu,¹ Eray Enustun,¹ Zeynep Ertuz,¹ Peter Scheiffele,⁵ Scott H. Soderling,^{1,6,7} Debra L. Silver,^{1,4,6,7} Ru-Rong Ji,^{3,6} Alexandre E. Medina,² and Cagla Eroglu^{1,6,7,*}

¹Department of Cell Biology, Duke University Medical Center, Durham, NC 27710

²Department of Pediatrics, University of Maryland, School of Medicine, Baltimore, MD 21201

³Department of Anesthesiology, Duke University Medical Center, Durham, NC 27710

⁴Department of Molecular Genetics and Microbiology, Duke University Medical Center, Durham, NC 27710

⁵Biozentrum University of Basel, 4056 Basel, Switzerland

⁶Department of Neurobiology, Duke University Medical Center, Durham, NC 27710

⁷Duke Institute for Brain Sciences (DIBS), Durham, NC 27710

⁸Co-first author

*Correspondence: sandeep.singh@duke.edu (S.K.S.), cagla.eroглу@dm.duke.edu (C.E.)

<http://dx.doi.org/10.1016/j.cell.2015.11.034>

SUMMARY

Proper establishment of synapses is critical for constructing functional circuits. Interactions between presynaptic neurexins and postsynaptic neuroligins coordinate the formation of synaptic adhesions. An isoform code determines the direct interactions of neurexins and neuroligins across the synapse. However, whether extracellular linker proteins can expand such a code is unknown. Using a combination of in vitro and in vivo approaches, we found that hevin, an astrocyte-secreted synaptogenic protein, assembles glutamatergic synapses by bridging neurexin-1 α and neuroligin-1B, two isoforms that do not interact with each other. Bridging of neurexin-1 α and neuroligin-1B via hevin is critical for the formation and plasticity of thalamocortical connections in the developing visual cortex. These results show that astrocytes promote the formation of synapses by modulating neurexin/neuroligin adhesions through hevin secretion. Our findings also provide an important mechanistic insight into how mutations in these genes may lead to circuit dysfunction in diseases such as autism.

INTRODUCTION

Neuronal communication flows through highly specialized cell junctions called synapses. *Trans*-synaptic adhesions between presynaptic neurexins (NRX) and postsynaptic neuroligins (NL) are critical for the formation and maturation of excitatory and inhibitory synapses (Baudouin and Scheiffele, 2010). Mutations in NRXs and NLs are linked to many neurological disorders, including autism, schizophrenia, depression, and addiction, highlighting the importance of this *trans*-synaptic link in normal brain function (Südhof, 2008).

NRXs are coupled to presynaptic vesicle release machinery, whereas NLs are linked to postsynaptic adaptor proteins and neurotransmitter receptors. Thus, NRX-NL pairs coordinate the organization and alignment of the pre- and postsynaptic specializations (Craig and Kang, 2007). In humans, there are three neurexin and five neuroligin genes. Each neurexin gene produces two isoforms, the long NRX α and the short NRX β . β -isoforms interact strongly with NLs, whereas α -isoforms have weak affinity toward NLs, in particular NL1 with a B-splice site insertion (NL1B) (Boucard et al., 2005; Chih et al., 2006; Graf et al., 2004). NRX α and NL1B isoforms are far more abundantly expressed in the brain (Schreiner et al., 2015). Recruitment of NRX α s, but not NRX β s, is key for the rapid induction of presynaptic release machinery at the sites of new axo-dendritic contacts (Lee et al., 2010), and NL1 is critical for recruiting NMDA-type glutamate receptors (NMDAR) to excitatory synapses (Budreck et al., 2013; Chubykin et al., 2007). These observations suggested the presence of synaptic linkers that align postsynaptic NMDARs with presynaptic release machinery via bridging of incompatible NRX α and NL1B.

Astrocytes, the most abundant glial cells of the brain, control synapse formation by secreting synaptogenic factors, including hevin/SPARCL1 (Kucukdereli et al., 2011; Risher et al., 2014). Hevin is a glycoprotein localized to the synaptic clefts of excitatory synapses (Johnston et al., 1990). Downregulation of hevin has been reported in neurological disorders such as autism and depression (Purcell et al., 2001; Zhurov et al., 2012), and copy number variations (CNV), polymorphisms, and mutations in *SPARCL1* are linked to autism and schizophrenia (De Rubeis et al., 2014; Jacquemont et al., 2006; Kahler et al., 2008). Hevin strongly stimulates excitatory synapse formation in the retinal ganglion cell (RGC) cultures and *Hevin* null mice (Hevin knockout [KO]) have fewer and immature excitatory synapses at the superior colliculus (SC), the synaptic target of RGCs in vivo (Kucukdereli et al., 2011). Moreover, in the developing cortex, hevin is required for proper thalamocortical synaptogenesis and the maturation of dendritic spine structures (Risher et al., 2014).

Despite hevin's fundamental role in excitatory synapse development in rodents and its potential association with neurological

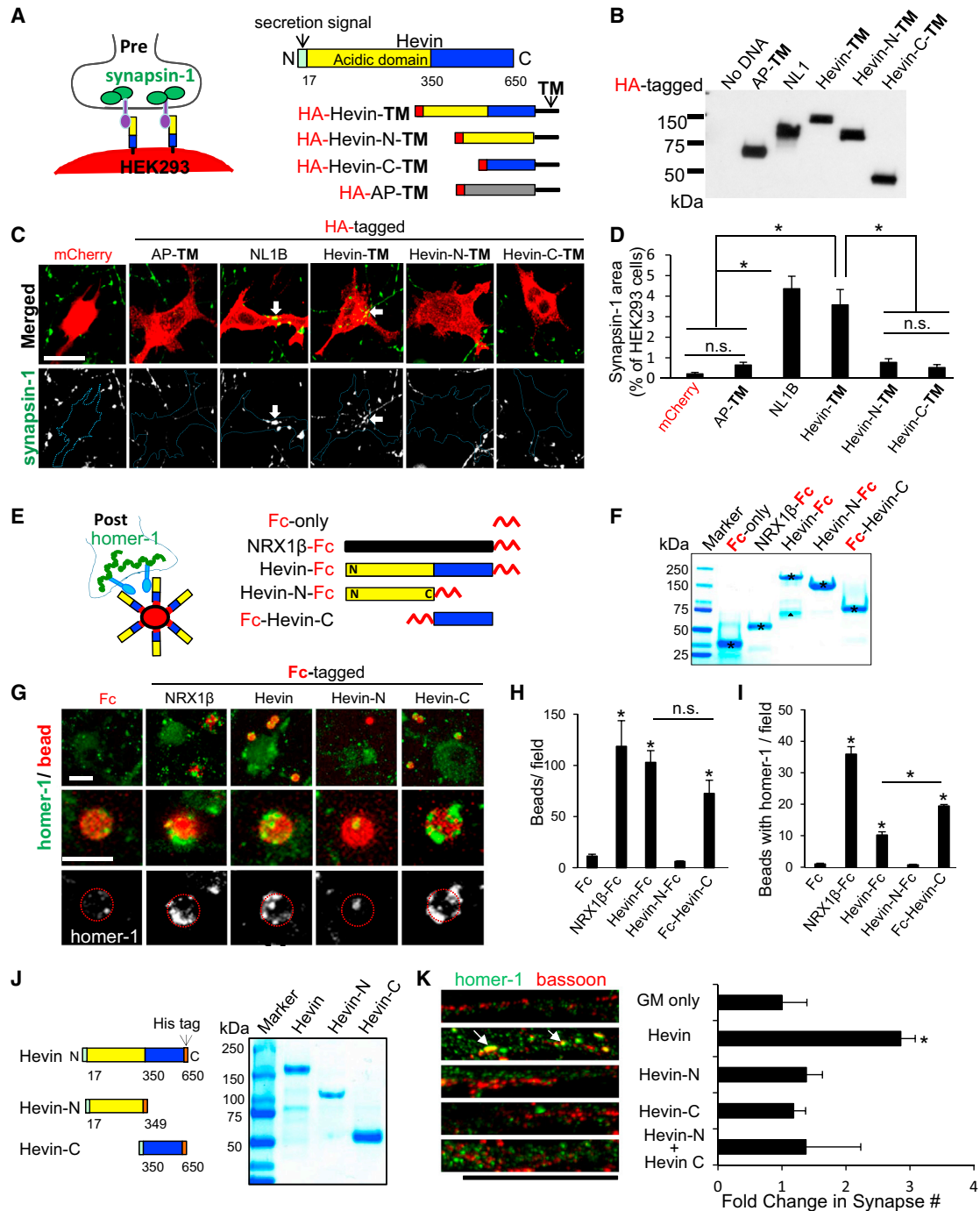


Figure 1. Hevin Organizes Pre- and Postsynaptic Specializations

(A) RGC-HEK293 co-culture assay. Trans-membrane-anchored (TM) and HA-tagged hevin and its fragments were expressed in HEK293 cells co-cultured with RGCs.

(B) Western blot analysis of the HEK293 expression of HA-tagged constructs.

(C) Representative images of synapsin-1 (green) clustering (arrow) on HA-tagged TM constructs expressed HEK293 cells (red). Scale bar, 20 μm.

(D) Quantification of the hemisynapse assay (n = 15–18 cells/condition) as the area of synapsin-1 on HEK293 cells (% HEK293 cell area).

(E) Schematic of the Fc-tagged proteins and homer-1-clustering in RGC-bead assay.

(F) SDS-PAGE analysis of pure Fc-tagged proteins (asterisk). In the Hevin-Fc lane a naturally occurring hevin cleavage product is also detected (triangle).

(G) Representative images of RGCs in the postsynaptic bead-clustering assay. Scale bars, 5 μm.

(H and I) Quantification of the number of beads/field (H) or beads with homer-1 clusters/field (I) (n = 10–15 fields/condition).

(legend continued on next page)

disorders in humans, how hevin induces synaptogenesis is unknown. Here, we show that hevin organizes pre- and postsynaptic specializations and induces thalamocortical synaptogenesis by bridging NRX1 α and NL1. Moreover, in the developing visual cortex, astrocyte-secreted hevin is required for the plasticity of thalamocortical connections. These results reveal that astrocytes alter the *trans*-synaptic interactions between NLs and NRXs via hevin and thus modulate the formation and plasticity of excitatory synapses. Because hevin (*SPARCL1*), NRX1 α (*NRXN1*), and NL1 (*NLGN1*) are all genetically linked to neurological disorders, our results also provide mechanistic insights into how mutations in these genes may lead to synaptic dysfunction in disease.

RESULTS

Hevin Organizes Pre- and Postsynaptic Specializations

Hevin induces the formation of ultrastructurally normal, but postsynaptically silent synapses (i.e., lacking AMPA receptors) between RGCs (Kucukdereli et al., 2011). However, hevin-induced synapses are presynaptically active as shown by live staining with luminal synaptotagmin antibody (Figures S1A and S1B). Moreover, hevin strongly enhances NMDA currents in autaptic RGC cultures suggesting it potentiates NMDA receptor function (Figures S1C–S1K). Because hevin affects both pre- and postsynapses in vitro and in vivo we postulated that hevin organizes pre- and postsynaptic specializations.

To determine whether hevin organizes presynaptic structures, we utilized a “hemisynapse” assay (Scheiffele et al., 2000). We engineered a membrane-anchored hevin construct (Hevin-TM), expressed it in HEK293 cells, and then co-cultured these cells with purified RGCs (Figures 1A–1D). Hevin-TM strongly induced clustering of presynaptic synapsin-1 puncta onto HEK293 cells (Figures 1C and 1D), but two negative controls: cells expressing (1) cytoplasmic mCherry or (2) alkaline phosphatase tethered to the cell membrane with the same TM-anchor did not (AP-TM; Figures 1A–1D).

Hevin has two distinct domains: a unique N-terminal acidic region followed by a secreted protein acidic and rich in cysteines (SPARC) homology region (Figure 1A). Metalloprotease ADAMTS4 cleaves hevin at amino acid 350, to produce N- and C-terminal fragments, which are found in the brain at low levels (Weaver et al., 2010). We tested presynaptic clustering ability of TM-tagged N- or C-terminal hevin fragments (Hevin-N-TM [17–349], Hevin-C-TM [350–650]) and found that neither induces synapsin-1 clustering onto HEK293 cells (Figures 1A–1D). Our findings show that hevin organizes presynaptic specializations and cleavage of hevin at amino acid 350 impairs its ability to organize presynapses.

Next, we tested whether hevin organizes postsynaptic specializations. We cultured RGCs with magnetic beads coated

with Fc-tagged full-length hevin or hevin-truncation constructs (Figures 1E and 1F). Hevin-Fc beads efficiently bound to neuronal processes and significantly induced homer-1 clustering compared to Fc-coated control beads (Figures 1G–1I). Deletion of the C terminus of hevin eliminated these functions (Hevin-N-Fc). In contrast, the C-terminal region of hevin (Fc-Hevin-C) efficiently bound to RGCs and strongly clustered homer-1 (Figures 1G–1I). These results show that the C terminus of hevin is sufficient to interact with neuronal processes and induce postsynaptic clustering. Collectively, our results show that hevin organizes both pre- and postsynaptic specializations.

To further understand the mechanism of hevin-induced synapse formation, we tested whether hevin truncation constructs (Figure 1J) were synaptogenic in RGC cultures. RGCs, cultured as a pure neuronal population, form few synapses as determined by the co-localization of pre- and postsynaptic markers (e.g., bassoon and homer-1, respectively; Figure 1K). Addition of hevin induces an \sim 3-fold increase in synapse number (Figure 1K, arrows). Even though the C terminus of hevin (Hevin-C) organizes postsynaptic specializations (Figures 1G–1I), neither Hevin-C alone, nor the co-application of Hevin-N and Hevin-C together mimicked full-length hevin’s synaptogenic effect (Figure 1K). These data suggest that simultaneous organization of pre- and postsynaptic sites by hevin is required for its synaptogenic effect.

NRX1 α and NLs Are the Pre- and Postsynaptic Receptors for Hevin

Similar to hevin, presynaptic NRXs and postsynaptic NLs organize pre- and postsynaptic specializations, respectively (Graf et al., 2004; Scheiffele et al., 2000). Thus, we postulated that hevin interacts with these receptors to induce synapse formation. There are four neuroligins (NL1–NL4) in rodents. We found that hevin co-immunoprecipitates (coIP) with NL1, NL2, and NL3 (Figure 2A). Knockdown of NLs 1–3 in RGCs using small hairpin RNAs (shRNA) completely abolished hevin-induced synaptogenesis in vitro, which was rescued by co-expression of shRNA-resistant human NL3 (hNL3; Figures 2B, 2C, and S2A). Individual knockdown of NLs 1–3 or in dual combinations all significantly reduced hevin-induced synaptogenesis (Figure S2B). These results show that NLs 1–3 are required for hevin-induced synapse formation in vitro.

We next tested whether hevin interacts with NRX1 isoforms (Figure 2D). We found that hevin coIP specifically with long NRX1 α but not with short NRX1 β (Figure 2E). Hevin did not coIP with NRX2 α and only weakly interacted with NRX3 α (Figure S2C), suggesting that hevin mainly interacts with NRX1 α . Additionally, the C-terminal domain of hevin, which interacts with NL1, had diminished interactions with NRX1 α (Figure 2F).

We found that hevin interacts in solution with Fc-tagged soluble NRX1 α extracellular domain (ECD) (Figures S2D–S2F). Bath application of the soluble NRX1 α -Fc with hevin at 1:1 molar ratio

(J) Purified full-length hevin or hevin fragments (5 μ g/lane).

(K) Left: representative images of RGC dendrites treated with growth media (GM) only, 80 nM hevin, or hevin fragments showing synapses as co-localization of bassoon and homer-1 (arrows). Scale bar, 20 μ m. Right: quantification of co-localized synaptic puncta/cell as fold change normalized to GM condition ($n > 20$ cells/condition).

For all graphs: * $p < 0.05$, one-way ANOVA followed by Fisher’s LSD post hoc test, error bars \pm SEM.

See also Figure S1.

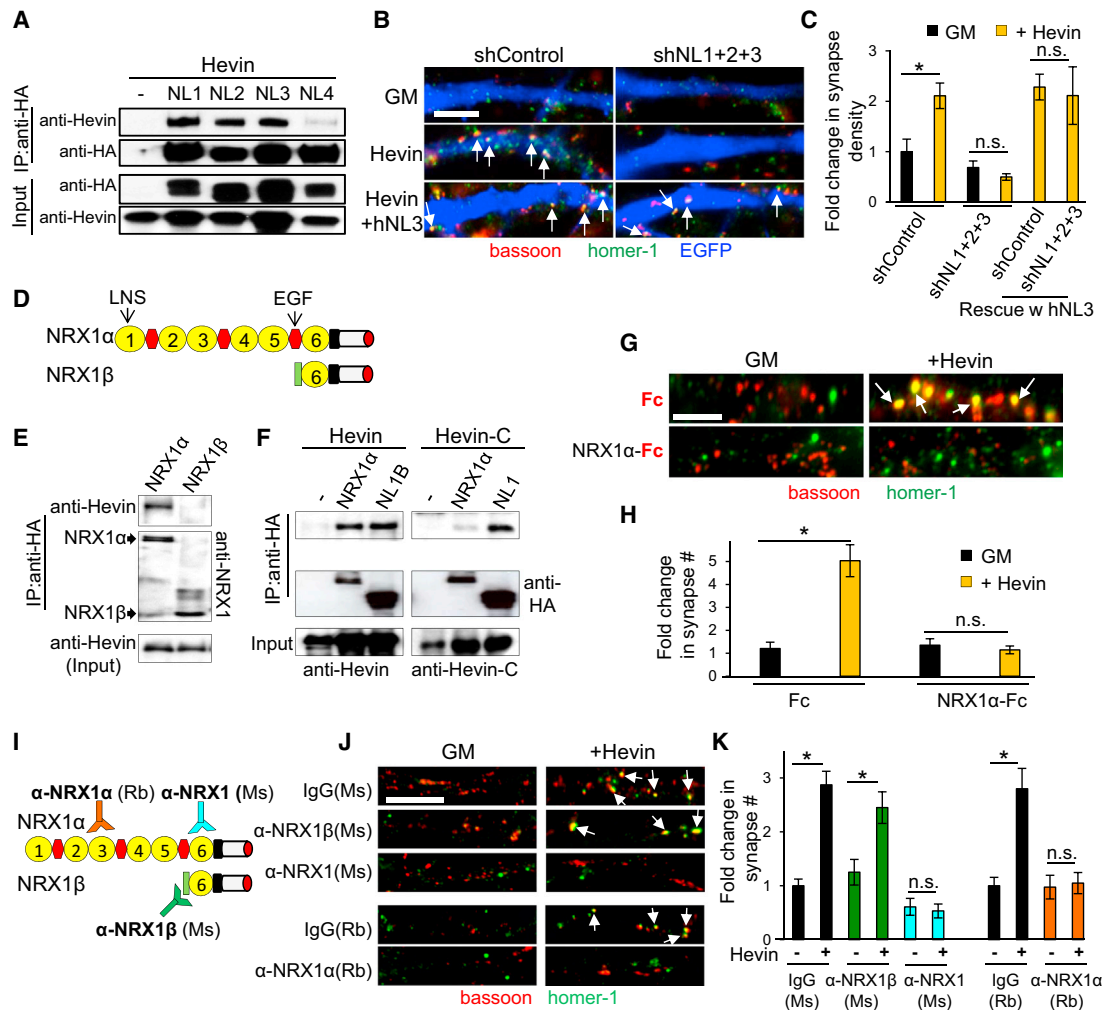


Figure 2. NLRs and NRX1 α Are Synaptic Receptors for Hevin

(A) Hevin co-immunoprecipitates (coIP) with HA-tagged NLRs in HEK293 cells.
 (B) Representative images of shRNA-transfected dendrite stretches (blue). Synapses are labeled as co-localized bassoon (red) and homer-1 (green) puncta.
 (C) Quantification of fold change in the density of synapses made onto transfected neurons as fold change normalized to the shControl-no hevin condition ($n > 40$ cells per condition). * $p < 0.05$; Student's *t* test; n.s., not significant, error bars \pm SEM.
 (D) Domain structures of NRX1 α and NRX1 β .
 (E) Hevin coIP with HA-tagged NRX1 α , but not with NRX1 β in HEK293 cells.
 (F) CoIP of Hevin-C fragment with NRX1 α and NL1.
 (G) Representative images of RGC dendrites treated with hevin and Fc-tagged proteins stained with bassoon (red) and homer-1 (green). Scale bar, 5 μ m.
 (H) Quantification of fold change in synapse number/cell normalized to the Fc-only treatment (3.2 ± 0.76 synapses in Fc-only condition, $n = 20$ cells/condition). * $p < 0.05$; Student's *t* test; n.s., not significant, error bars \pm SEM.
 (I) Schematic presentation of the epitope locations for anti-NRX1 antibodies.
 (J) Representative images of RGC dendrites with bath-applied NRX1-recognizing antibodies with or without hevin.
 (K) Quantification of fold change in synapse number/cell ($n > 28$ cells/condition, * $p < 0.05$; one-way ANOVA followed by Fisher's LSD post hoc test, error bars \pm SEM). Fold change is calculated by normalizing to the number of synapses/cell in respective Ms or Rb control antibody-only treated condition (2.72 ± 0.97 and 3.36 ± 0.16 synapses in Ms and Rb antibody-only condition, respectively). Scale bars, 5 μ m.
 See also Figure S2.

blocked hevin-induced synaptogenesis in vitro (Figures 2G and 2H), suggesting that the NRX1 α -hevin interaction is important for hevin's synaptogenic function. Next, we tested whether antibodies against NRX1 ECD (Figures 2I and S2G) can block hevin-induced synapse formation. A mouse monoclonal antibody recognizing α and β NRX1 or a rabbit polyclonal antibody against

an epitope specific for NRX1 α blocked hevin-induced synaptogenesis (Figures 2J and 2K). In contrast, a NRX1 β -specific monoclonal antibody did not block hevin-induced synaptogenesis (Figures 2J and 2K). Taken together, these data indicate that NRX1 α is the presynaptic receptor for hevin's synaptogenic function.

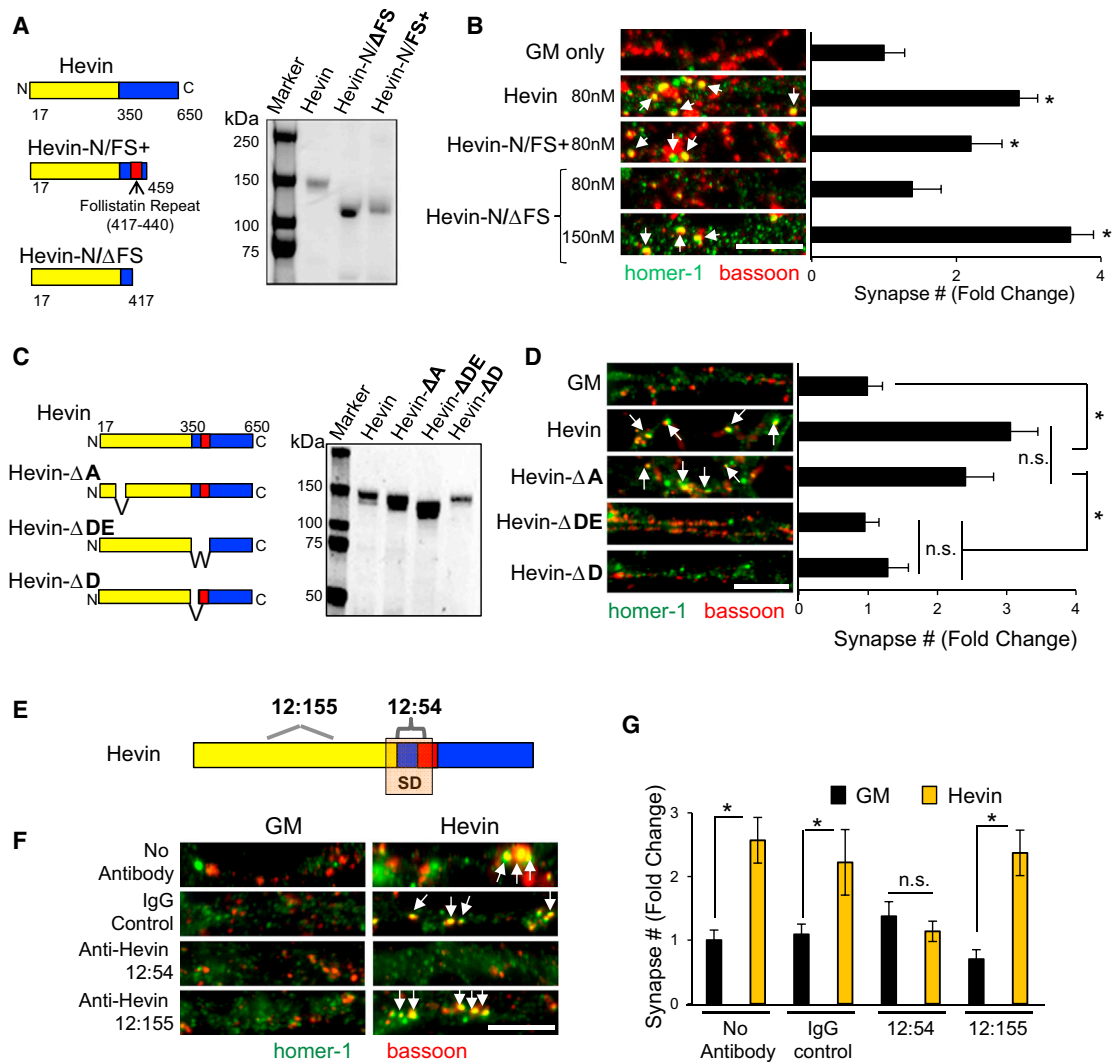


Figure 3. Identification of a Region within Hevin that Is Critical for Its Receptor Interactions and Synaptogenic Activity

(A) Domain organization and SDS-PAGE analysis of hevin and two synaptogenic hevin fragments.

(B) Representative images of RGC dendrites treated with GM or recombinant hevin proteins. Synapses are labeled as the co-localization of bassoon (red) and homer-1 (green) puncta (arrows). Data is presented as fold change in synapse number/cell compared to GM ($n > 35$ cells).

(C) Schematics and SDS-PAGE analysis of hevin and hevin deletion mutants.

(D) Representative images of RGC dendrites treated with GM, hevin or hevin deletion mutants, arrows point to co-localized synaptic puncta. Data is presented as fold change in synapse number/cell compared to GM ($n > 35$ cells).

(E) Schematic of hevin's putative synaptogenic region (SD) and epitopes for the two rat monoclonal antibodies against hevin.

(F) Representative images from dendrites of RGCs treated with GM or hevin in the presence of serotype matched control rat antibody (IgG-Control) or anti-Hevin 12:155 or anti-Hevin 12:54.

(G) Quantification of fold changes in synapse number/cell relative to GM condition (3.25 ± 0.84 synapses/cell, $n > 20$ cells/condition). * $p < 0.05$, one-way ANOVA followed by Fisher's LSD post hoc test error bars \pm SEM. Scale bars, 5 μ m.

See also Figure S3.

Identification of a Region within Hevin that Mediates Receptor Interactions and Synaptogenic Activity

Cleavage of hevin at amino acid 350 eliminates its synaptogenic function (Figure 1K). Thus, we postulated that a region surrounding the cleavage site is critical for hevin's synaptogenic interactions. Consistent with this, a hevin truncation construct spanning amino acids 17–459 (Hevin-N/FS+) induced synapse formation (Figures 3A and 3B) and interacted efficiently with NRX1 α and

NL1 (Figure S3A). In contrast, non-synaptogenic Hevin-N (Figure 1K) did not interact with NRX1 α and weakly interacted with NL1B (Figure S3A). Moreover, a hevin fragment (17–417) lacking the follistatin-like domain (Hevin-N/ΔFS) was synaptogenic only at higher concentrations (Figures 3A, 3B, and S3B) and interacted weakly with NRX1 α and NL1B (Figure S3A). Taken together, these data show that the first 459 amino acids of hevin mediate its synaptogenic activity and interact with both NRX1 α

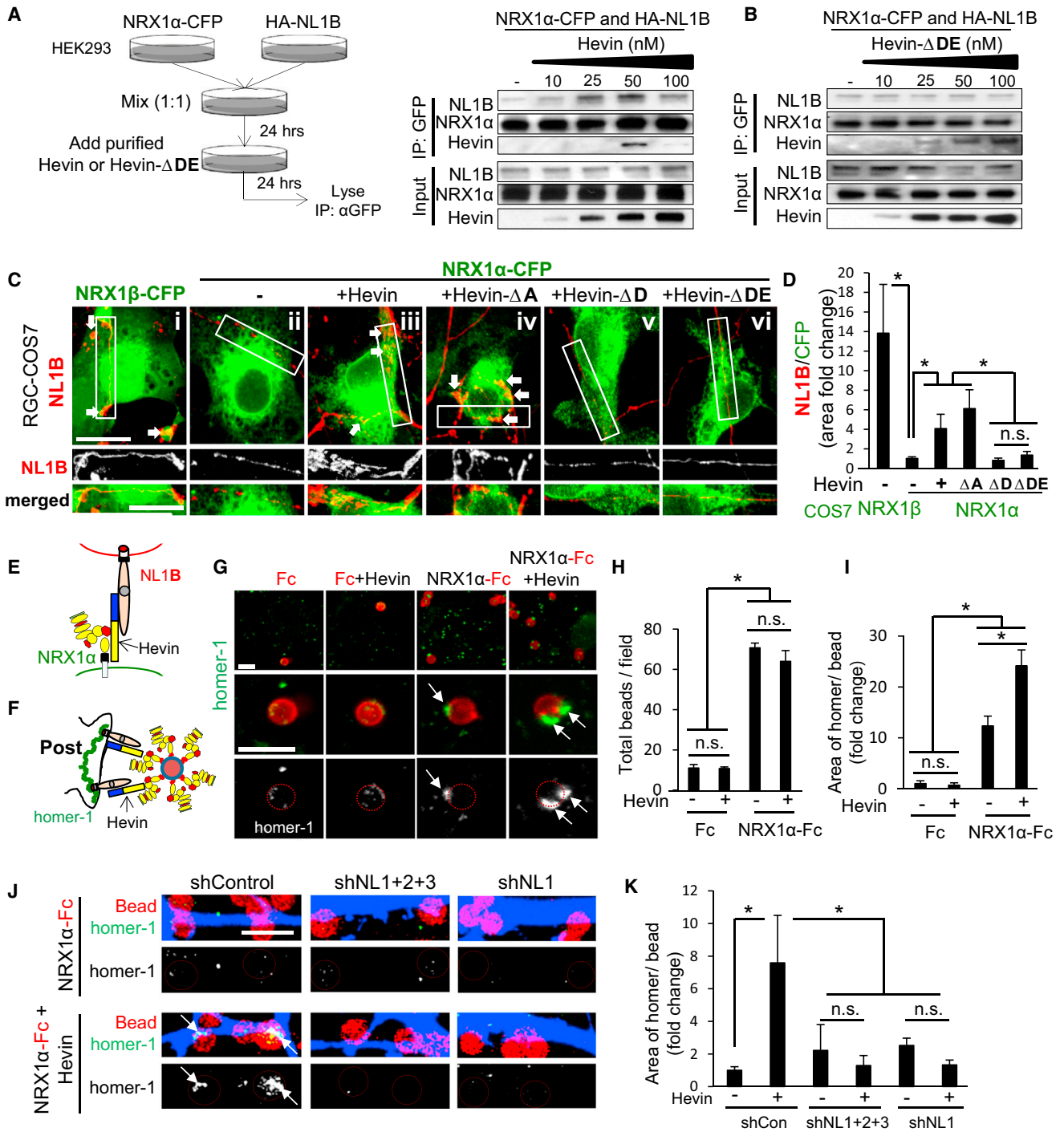


Figure 4. Hevin Bridges Interaction-Incompatible NRX1 α and NL1B Transcellularly

(A and B) Triple coIP strategy: HEK293 cells were transfected with NRX α or NL1 isoforms and cells were mixed in the presence of various hevin or Hevin- Δ DE concentrations. Western blot analyses of the effects of hevin (A) or Hevin- Δ DE (B) on NRX1 α /NL1B interactions.

(C) Representative images of the co-clustering of CFP-tagged α or β NRX1-expressing COS7 cells (green) co-cultured with HA-NL1B expressing RGCs (red). Scale bar, 10 μ m.

(D) Quantification of NL1B clustering onto NRX1-expressing COS7 cells. Data presented as fold change of the ratios of NL1B area per NRX1-expressing cell area (n = 15–38 cells per condition) normalized to NRX1 α -CFP expressing cells in GM condition.

(E) Hevin can bridge incompatible NRX1 α and NL1B transcellularly.

(F) Schematic presentation of the NRX1 α -bead assay.

(legend continued on next page)

and NL1B efficiently. The follistatin-like domain of hevin is not essential for its synaptogenic function, but plays a role in strengthening hevin-receptor interactions. Our findings also show that the region around amino acids 350–417 of hevin is critical for its synaptogenic activity.

Next, we mapped two putative NRX1 α and NL1B interaction sites within amino acids 350–440 of hevin by using a peptide array (Figures S3C and S3D). We named these sites as D and E, based on their location on the arrays (Figure S3C). We produced three hevin-deletion mutants: (1) Hevin- Δ DE (lacking 351–440), (2) Hevin- Δ D (lacking 351–372), and (3) Hevin- Δ A (lacking 88–115, removing another putative interaction site for NRX1 α) (Figure 3C and S3D). We found that Hevin- Δ A was synaptogenic like hevin; however, Hevin- Δ D and Hevin- Δ DE did not induce synapse formation *in vitro* (Figure 3D) even at higher concentrations (Figure S3E). This result shows that the putative NRX1 α and NL1B interaction sites within 351–440 are critical for hevin's synaptogenic function.

Consistent with this, a rat monoclonal antibody against an epitope within amino acids 368–419 of hevin (anti-hevin 12:54) blocked hevin's synaptogenic function, when co-applied to RGCs with hevin (Figures 3E–3G). Another rat anti-hevin antibody (12:155), with epitopes within the N-terminal acidic domain of hevin (epitopes: 117–123 and 245–251, Figures 3E–3G) did not block hevin-induced synaptogenesis. Collectively, these results show that a region at the cusp of hevin's N- and C-terminal domains is critical for hevin's synaptogenic function.

Hevin Bridges NRX1 α and NL1B Transcellularly

NRX1 α interacts strongly with the A-site containing NL1, but weakly with the B-site containing splice variant, NL1B (Chih et al., 2006; Siddiqui et al., 2010). As hevin interacts with both NRX1 α and NL1B, hevin might bridge these two receptors and enable their interaction. In agreement, hevin facilitated the co-immunoprecipitation of NRX1 α and NL1B in a concentration-dependent manner (Figure 4A), whereas neither the weak interaction between NRX2 α and NL1B nor the strong interaction between NRX1 α and NL1A were altered by hevin (Figures S4A and S4B). Interestingly, tripartite complex formation is impaired at hevin concentrations beyond its optimal synaptogenic dose (>100 nM; Figure S3E), and the non-synaptogenic Hevin- Δ DE did not facilitate the interaction between NRX1 α and NL1B (Figure 4B). These data suggest that hevin enhances the interaction between NRX1 α and NL1B via its synaptogenic region.

RGCs and their synaptic target SC predominantly express the interaction incompatible NRX1 α and NL1B (Figures S4C and S4D). Therefore, we tested whether hevin bridges NRX1 α and NL1B transcellularly, using an “RGC-COS7 co-culture assay.” COS7 cells expressing CFP-tagged (green) NRX1 α or

NRX1 β were co-cultured with HA-NL1B-expressing RGCs (red) (Figure 4C). NL1B-expressing neurites strongly interacted with NRX1 β -CFP-expressing COS7 cells (Figures 4Ci and 4D, arrows), but did not with NRX1 α -CFP-expressing cells (Figures 4Cii and 4D). However, NRX1 α -CFP-expressing COS7 cells recruited an interaction-compatible postsynaptic partner, LRRTM2 (Figure S4E). Application of soluble hevin strongly promoted the clustering of NL1B onto NRX1 α -CFP-expressing COS7 cells (Figures 4Ciii and 4D), showing that hevin bridges the interaction-incompatible NRX1 α and NL1B transcellularly (Figure 4E). Similarly, in a “HEK293 cell aggregation” assay hevin induced aggregation of NL1B and NRX1 α -expressing cells (Figures S4F–S4H, arrow), but did not alter the aggregation of compatible NL1A and NRX1 α -expressing cells (Figure S4H).

To determine if hevin's synaptogenic activity depends on its ability to bridge NRX1 α and NL1B, we tested hevin deletion mutants in the same transcellular bridging assays. Synaptogenic Hevin- Δ A efficiently bridged NRX1 α and NL1B in both assays, whereas non-synaptogenic Hevin- Δ D and - Δ DE did not (Figures 4Civ–4Cvi, 4D, S4I, and S4J). In summary, our data show that hevin can bridge incompatible NRX1 α and NL1B transcellularly and that bridging is required for its synaptogenic activity. These results reveal that hevin may act as a *trans*-synaptic linker to assemble excitatory synapses.

Hevin Recruits NL1 and Associated Postsynaptic Proteins to Excitatory Synapses

Collectively our results suggest that hevin may facilitate the recruitment of NL1-associated proteins, such as PSD95 and homer-1, by bridging NRX1 α and NL1. To test this, we added NRX1 α -Fc coated beads onto the cultured RGCs in the presence or absence of hevin (Figure 4F). These beads bound to RGC somas and dendrites (Figure 4G). Hevin did not alter bead attachment efficiency (Figures 4G and 4H), but strongly enhanced (2- to 8-fold) the homer-1 recruitment to the beads (Figures 4G–4K). Silencing NLRs 1-3 or only NL1 in RGCs, abolished hevin's recruitment of homer-1 by NRX1 α (Figures 4J and 4K). In sum, these results show that hevin organizes postsynaptic structures by linking NRX1 α and NL1.

These data indicate that hevin recruits NL1 and NL1-associated proteins to synapses. In agreement, NL1, PSD95, homer-1, and the NMDAR subunits NR1 and NR2B levels were significantly reduced in the postsynaptic membranes of Hevin KO cortices compared to wild-type (WT) (Figure S5A). Moreover, hevin and NL1 co-localize in the mouse cortex (Figures S5B and S5C) and NL1 staining is greatly reduced in the upper cortical layers (1–4) of Hevin KO mice (Figure S5D). The reduction in NL1 is not due to a gross morphological abnormality in the cortices of Hevin KOs, because these mice have normal

(G) Representative images of analyzed fields (top) or single beads (middle and bottom) showing homer-1 (green) clustering on NRX1 α -Fc-coated beads (red) in the presence or absence of hevin. Scale bar, 5 μ m.

(H and I) Quantification of the number of beads/field (H) and fold change in the area of homer-1 clusters per bead (I) ($n = 10$ –15 fields/condition) normalized to the NRX1 α -Fc beads without hevin condition.

(J) Representative images of shRNA-transfected dendrites (blue) stained for homer-1 (green) and beads (red circles). Scale bar, 5 μ m.

(K) Quantification of the area of homer-1 clusters per bead ($n = 10$ fields/condition) as fold change normalized to the shControl no hevin condition. * $p < 0.05$ one-way ANOVA followed by Fisher's LSD post hoc test, error bars \pm SEM.

See also Figures S4 and S5.

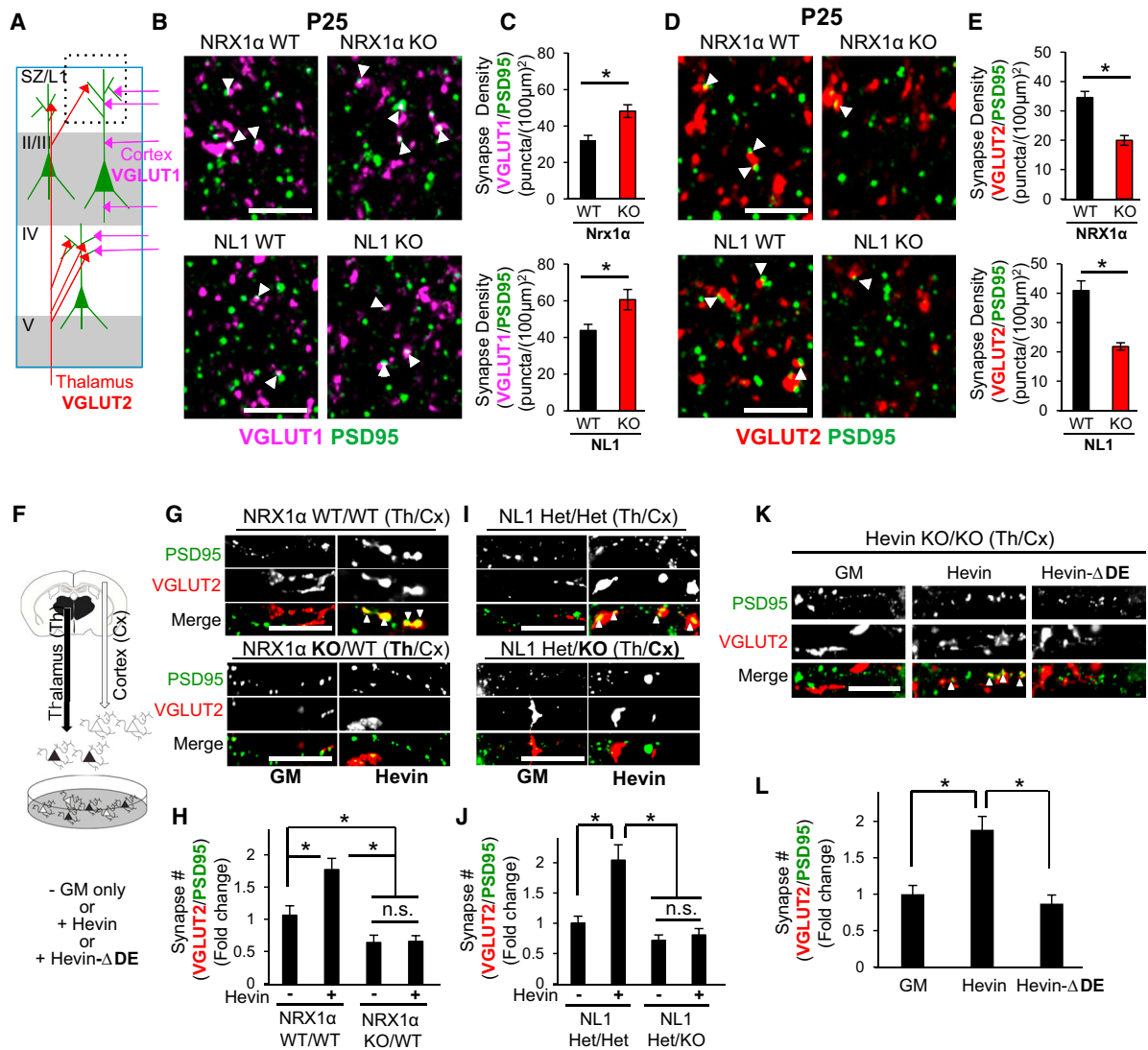


Figure 5. NRX1 α and NL1 Are Required for Thalamocortical Synapse Formation

(A) Excitatory synaptic circuitry within the mouse V1 cortex. Synapse density analysis was performed in the synaptic zone (SZ/L1, dashed black box). (B and D) Representative zoomed-in images of P25 NRX1 α (top) or NL1 (bottom) WT and KO V1 cortices stained for (B) VGLUT1 (magenta) and PSD95 (green) or (D) VGLUT2 (red) and PSD95. Scale bar, 5 μ m. (C and E) Quantification of (C) VGLUT1/PSD95 or (E) VGLUT2/PSD95 synapse density in NRX1 α (top) or NL1 (bottom) littermate WT and KO mice (n = 3 mice/genotype). Data are represented as mean synaptic density per (100 μ m)² \pm SEM. *p < 0.05, Student's t test. (F, G, and I) Schematic of thalamocortical co-culture experiments. Representative images of dendrite segments treated with or without hevin (80 nM) from (G) WT cortical (Cx) neurons co-cultured with NRX1 α WT or KO thalamic (Th) neurons or (I) NL1 HET or KO cortical (Cx) neurons co-cultured with NL1 HET thalamic (Th) neurons. Co-localization of VGLUT2 (red) and PSD95 (green) mark thalamocortical synapses (arrowheads). Scale bar, 5 μ m. (H and J) Quantification of fold change in VGLUT2/PSD95 positive synapse number/cell normalized to the number of synapses (H) in NRX1 α WT/WT (Cx/Th) cultures without Hevin or (J) in NL1 HET/HET (Cx/Th) cultures without Hevin. (K) Representative images of dendrite segments from cortical neurons in thalamocortical co-cultures prepared from Hevin KO mice with or without hevin or Hevin- Δ DE (80 nM). (L) Quantification of VGLUT2/PSD95 synapse numbers/cell normalized to GM condition. (H, J, and L) n > 30 cells/condition, *p < 0.05; one-way ANOVA followed by Fisher's LSD post hoc test, error bars \pm SEM. See also Figure S6.

neuronal distribution and outgrowth in the cortex (Figure S5E) (Risher et al., 2014).

The presynaptic vesicular glutamate transporters VGLUT1 and VGLUT2 mark two major classes of cortical excitatory syn-

apses, the intracortical and thalamocortical, respectively (Figure 5A). NL1 puncta are closely apposed to subsets of VGLUT1 and VGLUT2 terminals in WT mice (Figures S5F and S5K), but Hevin KO cortices have a severe loss of NL1 puncta and

NL1/VGLUT apposition in the upper cortical layers (Figures S5G–S5J and S5L). The abundance of NL1 and VGLUT proteins are not significantly different in WT and littermate KO mice (Figures S5M and S5N). Collectively, these data show that hevin is required for the proper localization of NL1 to cortical excitatory connections.

Hevin Assembles Thalamocortical Synapses by Bridging NRX1 α and NL1

Hevin is required for proper cortical synaptic connectivity in mice. Hevin KO mice display a profound loss of VGLUT2⁺ thalamocortical synapses, which is offset by an increase in VGLUT1⁺ intracortical connections (Risher et al., 2014). Similar to Hevin KO mice, both NRX1 α and NL1 KO mice had significantly higher numbers of VGLUT1⁺ synapses (Figures 5B, 5C, S6A, and S6B), coupled with a strong reduction in VGLUT2⁺ synapses compared to their WT littermates (Figures 5D, 5E, S6C, and S6D). The reduced thalamocortical synapse numbers in NRX1 α and NL1 KO mice are not due to diminished axonal innervation of V1 by thalamic inputs from the dorsal lateral geniculate nucleus (dLGN) (Figures S6E–S6G). The total number of glutamatergic excitatory synapses was not significantly different between NRX1 α or NL1 KO mice compared to their littermate controls (Figures S6H and S6I). These findings show that NRX1 α and NL1 are required for proper thalamocortical synapse formation, suggesting that hevin induces thalamocortical synaptogenesis via its interactions with NRX1 α and NL1.

In a purified cortical and thalamic neuron co-culture system (Figure 5F), hevin specifically induces VGLUT2⁺ thalamocortical synapse formation onto cortical neurons (Risher et al., 2014). Interestingly, thalamic neurons predominantly express NRX1 α , whereas cortical neurons make NL1B (Figures S6L and S6M). Thus, hevin may induce thalamocortical synaptogenesis by bridging NRX1 α and NL1B. In agreement, we found that when the thalamic neurons lack NRX1 α , hevin cannot induce VGLUT2⁺ synapse formation (Figures 5G and 5H). Concordantly, the lack of NL1 in cortical neurons abolished hevin-induced thalamocortical synapse formation in vitro (Figures 5I and 5J). Moreover, Hevin- Δ DE, which cannot bridge NRX1 α and NL1B, did not induce thalamocortical synaptogenesis in co-cultures prepared from Hevin KO mice (Figures 5K and 5L). Taken together these data show that hevin-induced thalamocortical synaptogenesis requires NRX1 α in thalamic and NL1 in cortical neurons and requires hevin's ability to bridge these two receptors transcellularly.

Reduced thalamocortical connectivity in Hevin KO mice can be rescued by injection of purified hevin into the cortex (Risher et al., 2014). Using the same assay, we found that hevin could not induce thalamocortical synaptogenesis when injected to NL1 KO mice, although it could trigger a significant synaptogenic response in heterozygous littermates (HET) (Figures 6A–6D).

To determine if bridging of NRX1 α and NL1 by hevin is critical for thalamocortical synapse formation in vivo, we injected pure hevin or Hevin- Δ DE into the cortices of Hevin KO mice. Importantly, hevin, but not Hevin- Δ DE, strongly induced the formation of thalamocortical synapses (Figures 6E and 6F). Taken together our results demonstrate that hevin induces thalamocortical synapse

formation by bridging its pre- and postsynaptic receptors, NRX1 α and NL1, respectively.

Astrocyte-Secreted Hevin Is Required for Ocular Dominance Plasticity

Ocular dominance plasticity (ODP) is a model of cortical plasticity based on visual experience-dependent functional and anatomical changes in V1 cortex during a critical period of development. Stimulating each eye elicits responses in the binocular zone of V1 (V1B) that can be recorded as visually evoked field potentials (VEPs) (Figure 7A). Most V1B neurons have a bias toward the thalamic inputs that relay information from the contralateral eye (Figure 7B). The ratio of VEP amplitudes triggered by the contralateral eye versus the ipsilateral eye produces a contralateral bias index (CBI), which in rodents is typically between 1.2–2.5 (Frenkel and Bear, 2004; Porciatti et al., 1999). During a critical period in development, monocular deprivation (MD) of the contralateral eye reduces CBI (Sawtell et al., 2003). This phenomenon, known as ODP, is dependent on NMDARs (Bear et al., 1990; Roberts et al., 1998).

Because hevin induces the formation of thalamocortical synapses and because Hevin KO mice have reduced levels of synaptic NR1 subunit (Figure S5A), an essential component for NMDAR function, here we tested whether Hevin KO mice have impaired ODP. After 7 days of MD, CBIs were significantly reduced in WT and Hevin HETs as expected (Figures 7D and 7E). However, CBIs did not change in Hevin KO mice (Figure 7F), showing that hevin is required for ODP.

To test whether hevin expression by developing cortical astrocytes is critical for ODP, we injected Hevin KO mice with adeno-associated viruses (AAV), that express hevin specifically in the astrocytes, into V1B at P3 (Figures 7G and 7H). Remarkably, hevin expression by V1B astrocytes fully rescued ODP in Hevin KO mice (Figure 7I). While the amplitude of VEPs of the contralateral eye was not significantly different between groups (Figure 7J), we noted a higher contralateral bias in Hevin KO mice, which returned to normal levels after hevin expression was rescued in astrocytes (Figure 7K).

Taken together, our findings show that the lack of hevin leads to deficits in neuronal plasticity during cortical development. Re-expression of hevin, specifically in astrocytes of V1B, is sufficient to rescue the plasticity defect in Hevin KO mice, demonstrating that secretion of hevin by astrocytes is critical for the assembly of thalamocortical circuits amenable to experience-dependent plasticity.

DISCUSSION

Astrocyte-Secreted Hevin Induces Synapse Formation by Bridging NRX1 α and NL1B

During brain development astrocytes actively provide signals that control synaptic connectivity (Chung et al., 2015). Here, we show that astrocyte-secreted hevin is a *trans*-synaptic linker that bridges presynaptic NRX1 α with postsynaptic NL1B. This way, hevin organizes both pre- and postsynaptic specializations and aligns them across the synapse. Importantly, these results show that astrocytes can control the formation and maturation of synaptic contacts by altering the interaction code between

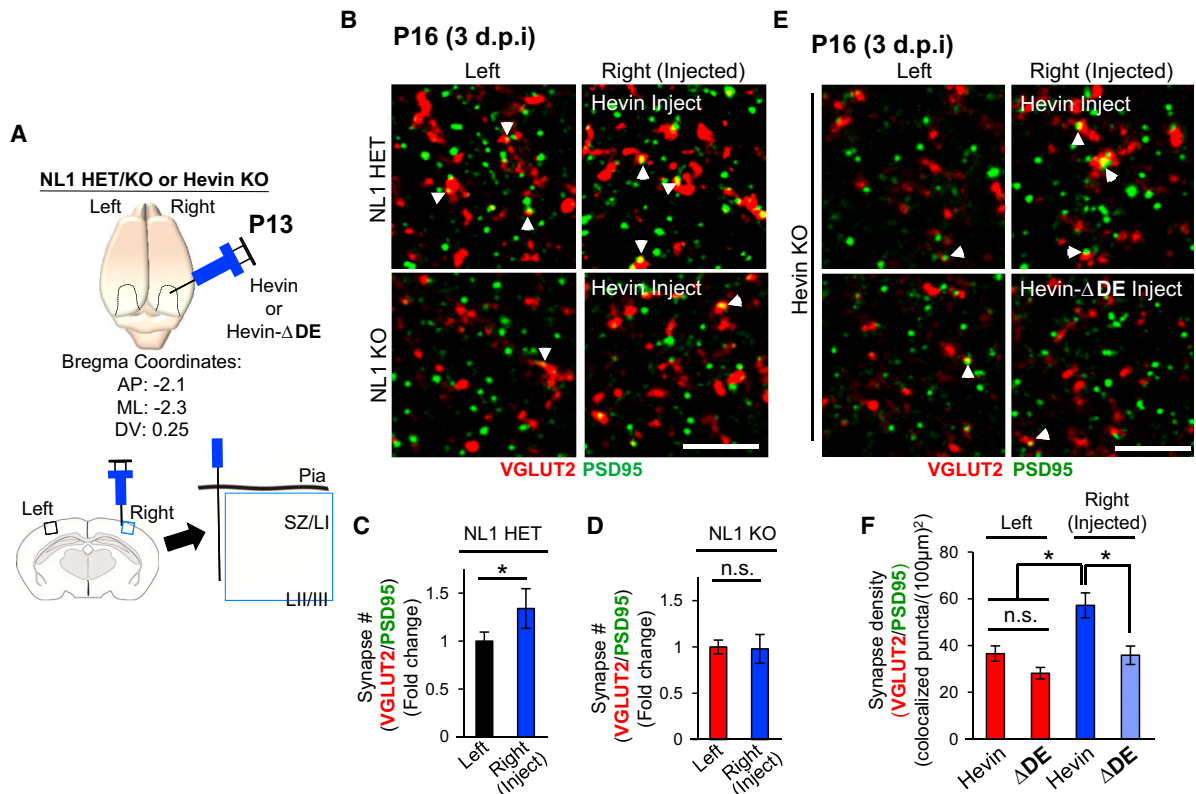


Figure 6. Hevin Induces Thalamocortical Synapse Formation In Vivo by Bridging NL1 and NRX1 α

(A) Schematics of in vivo hevin or Hevin- Δ DE injection experiments into the cortices of P13 NL1 HET/KO or Hevin KO mice at the indicated bregma coordinates. Imaging and analysis for VGLUT2/PSD95 was limited to the SZ just outside of the injection site (blue box).

(B and E) Representative zoomed-in images of synaptic staining in left (uninjected) and right (injected) hemispheres of (B) NL1 HET and KO littermates or (E) Hevin KOs. Thalamocortical synapses are visualized by the VGLUT2/PSD95 colocalization (arrowheads). Scale bar, 5 μ m.

(C and D) Quantification of VGLUT2/PSD95 synapses in NL1 HET or KO brains. Data presented as fold change in synapse number normalized to the number of synapses of the uninjected (left) hemisphere. * $p < 0.05$, Student's t test; n.s., not significant, $n = 3$ mice/genotype. Synapse density in the left (uninjected) cortices of NL1 HETs (78.87 ± 6.96 VGLUT2/PSD95 puncta/(100 μ m²) and KOs (48.88 ± 3.01 VGLUT2/PSD95 puncta/(100 μ m²) were significantly different from each other ($p = 0.0002$).

(F) Quantification of thalamocortical synapse densities in Hevin KOs injected with hevin or Hevin- Δ DE. Data are presented as mean synaptic density per (100 μ m²) \pm SEM. * $p < 0.05$, one-way ANOVA followed by Fisher's LSD post hoc test.

pre- and postsynaptic cell adhesion proteins. Astrocytes thereby modulate the abundance of specific *trans*-synaptic adhesion complexes and their associated receptors at synapses. Through hevin, astrocytes orchestrate the assembly of excitatory *trans*-synaptic adhesion complexes that contain NRX1 α and NL1, into larger adhesions, strengthening the synaptic junctions (Figure S7). This organization is critical for the formation and plasticity of thalamocortical synapses in the developing cortex.

How Does *trans*-Synaptic Bridging of NRX1 α and NL1B by Hevin Control Synapse Formation and Plasticity?

In addition to their *trans*-synaptic interactions, NRX1 α recruits presynaptic release machinery to the synapse (Lee et al., 2010; Missler et al., 2003); whereas, NL1 recruits NMDARs to postsynapses (Chubykin et al., 2007). By *trans*-synaptically linking NRX1 α and NL1B, hevin could align the neurotransmitter release machinery with the NMDARs. This alignment might be critical for the recruitment of NMDARs to the synapse, because the levels of

NR1 and NR2B at postsynaptic membranes were severely reduced in the Hevin KOs, and hevin strongly enhanced NR2B-containing NMDAR currents in autaptic RGC cultures. NL1 recruits NR1-subunit of NMDARs through extracellular interactions (Budreck et al., 2013), but how NRX1 α /hevin/NL1 interaction specifically recruits NR2B-containing NMDARs to the synapses remains to be elucidated.

The necessity of hevin for proper synaptic recruitment of NMDARs may also underlie its requirement for cortical plasticity. NMDAR is crucial for activity-dependent plasticity, by acting as a "coincidence detector" (Bourne and Nicoll, 1993; Huang et al., 2005). ODP (Bear et al., 1990; Roberts et al., 1998) as well as binocular recovery from monocular deprivation (Krahe and Binocular, 2010) require this feature of NMDAR function. Thus, by bridging NRX1 α and NL1, hevin may recruit NMDARs to thalamocortical synapses enabling plasticity of these connections.

There was a modest, but significant, increase in the CBI of the Hevin KOs. A sharp reduction in ipsilateral inputs leads to a

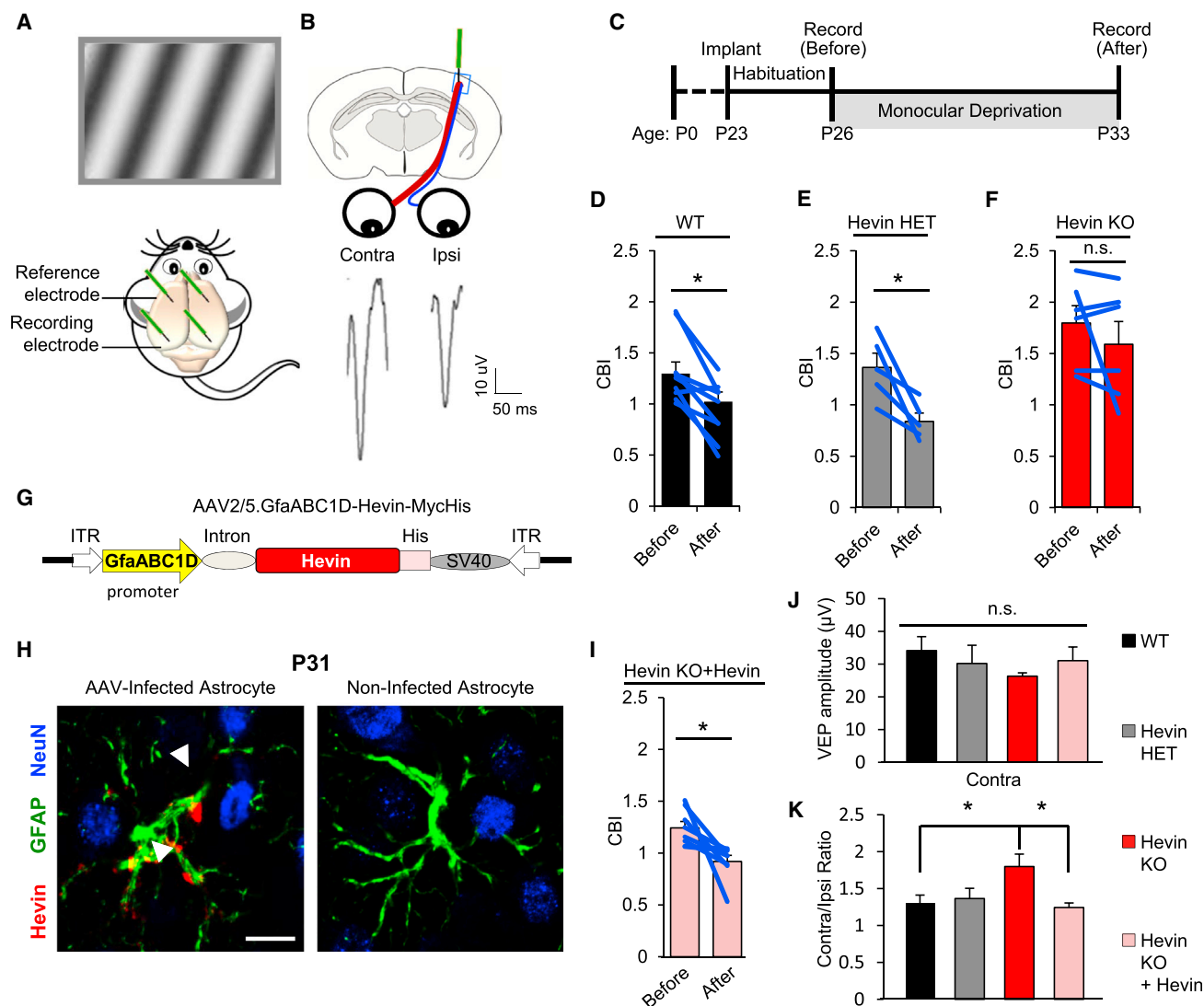


Figure 7. Astrocyte-Secreted Hevin Is Required for Ocular Dominance Plasticity

(A) Mice were implanted with recording electrodes in layer 4 of the V1B cortex. A visual stimulus is displayed to mice while visually evoked potentials (VEPs) are recorded.

(B) Cartoon schematic and VEP tracings from independent eye stimulations.

(C) Experimental timeline used to study ocular dominance plasticity (ODP).

(D–F) Contralateral bias indices (CBI) before and after monocular deprivation (MD). Data are presented as mean CBI \pm SEM. * $p < 0.05$; paired t test; n.s., not significant.

(G) AAV2/5-GfaABC1D-Hevin-myc-His viral construct used for astrocyte-specific rescue of hevin expression.

(H) Hevin (red) expression is driven specifically in astrocytes (GFAP⁺, green), but not in neurons (NeuN⁺, blue). Scale bar, 10 μ m.

(I) Astrocyte-specific hevin expression fully rescues ODP in Hevin KO mice. Data are presented as mean CBI \pm SEM. * $p < 0.05$; paired t test.

(J) Absolute VEP amplitude does not differ between all groups. * $p < 0.05$; one-way ANOVA followed by Fisher's LSD post hoc test.

(K) Comparison of CBIs before MD. Data are presented as mean CBI \pm SEM. * $p < 0.05$; one-way ANOVA followed by Fisher's LSD post hoc test.

severe increase in CBI, which can affect the development of retinotopy (Smith and Trachtenberg, 2007). However, this seems unlikely here as the CBIs of Hevin KO mice are in the range of what is commonly seen in mice (Coleman et al., 2009; Frenkel and Bear, 2004; Porciatti et al., 1999), which exhibit ODP. Moreover, re-expression of hevin in astrocytes by AAVs rescued this difference in CBI as well as the ODP.

How Do NRX1 α -Hevin-NL1 Interactions Dynamically Regulate Synaptic Connectivity?

Fine astrocyte processes, positioned next to synaptic clefts, can detect neurotransmitter release in nearby synapses. It is thought that in response to changes in synaptic activity patterns, astrocytes signal back to the synapse to modulate transmission or alter plasticity (Chung et al., 2015). It is plausible that hevin is

provided to the synaptic clefts of certain synapses in an activity-dependent manner to specifically bridge NRX1 α and NL1B. Future studies investigating how hevin secretion is regulated and whether synaptic activity can change hevin abundance in the brain are necessary.

Besides directional release from astrocytes, hevin's activity may be regulated by metalloproteases that cleave the protein into N- and C-terminal fragments (Weaver et al., 2010). Our findings show that this cleavage renders hevin inactive by impairing its ability to link NRX1 α and NL1B. Moreover, glial cells express a close homolog of hevin, called SPARC. SPARC is not synaptogenic, but blocks the synaptogenic activity of hevin (Kucukdereli et al., 2011). SPARC expression is altered by sensory experience (Tropea et al., 2006). Therefore, changes in SPARC abundance could dynamically regulate hevin activity. How SPARC blocks hevin-induced synaptogenesis remains to be elucidated.

Role of Astrocyte-Neuron Signaling via Hevin in Neurological Disorders

Alterations in synaptic development and function underlie the pathophysiology of many neurological disorders, including addiction, depression, schizophrenia, and autism. Therefore, an important implication of our findings is that perturbations in the NRX1 α -hevin-NL1 interaction could play a critical role in the synaptic pathologies seen in these disorders. In agreement with this, hevin (*SPARCL1*), NRX1 α (*NRXN1*), and NL1 (*NLGN1*) are linked to these diseases.

In a study on the molecular mechanisms of resilience, the injection of viruses that express hevin reversed the effects of social defeat in mice by promoting resilience and acted in an antidepressant-like fashion (Vialou et al., 2010). Moreover, hevin mRNA is one of the most downregulated transcripts in the brains of suicide victims compared to age-matched controls and hevin expression is reduced in the brains of depressed individuals (Zhurov et al., 2012), indicating that modulation of NRX1 α -hevin-NL1 interactions may provide fruitful new avenues for treatment or prevention of these mood disorders.

A comprehensive whole-genome sequencing of autistic individuals, identified *SPARCL1* gene mutations (ranking 35th among 107 high risk genes identified) (De Rubeis et al., 2014). The same study and others also identified *NRXN1*, *NLGN1*, *GRIN1* (NR1), and *GRIN2B* (NR2B) as autism risk genes. Thus, our findings, showing that these proteins work in concert to establish proper thalamocortical connectivity, provide an important mechanistic insight into how mutations in these genes may lead to synaptic dysfunction in autism. In fact, abnormal thalamocortical connectivity has been reported in autism patients (Nair et al., 2013). Future studies investigating the role of hevin in the pathophysiology of neurological disorders could determine if the modulation of synaptic adhesions by hevin, and its receptors can provide a molecular mechanism that could be exploited for therapeutic strategies.

EXPERIMENTAL PROCEDURES

All animals were used in accordance with Institutional Animal Care and Use Committee (IACUC) and Duke Division of Laboratory Animal Resources

(DLAR) oversight. Detailed experimental procedures can be found in the [Supplemental Experimental Procedures](#).

RGC Culture System to Study Synapse Formation In Vitro

RGCs were purified and cultured as previously described (Kucukdereli et al., 2011). After 4 days in vitro (DIV) purified recombinant hevin (WT or mutants) were added for an additional 6 days. Synapse quantification in RGC cultures were performed as described in Ippolito and Eroglu (2010).

DNA Constructs and Protein Purification

Hevin, hevin truncation, and deletion mutants were all cloned into pAptag5 vector. Recombinant proteins were purified from conditioned media of transfected HEK cells by using Ni-NTA resin (QIAGEN). Plasmid constructs for NLs and NRXs were described in (Chih et al., 2005, 2006; Graf et al., 2004; Siddiqui et al., 2010). TM fusion constructs: cDNA encoding the transmembrane region of LDL-TM and the cytoplasmic tail of CD46 was cloned into AP or hevin fragment containing pAptag5 plasmids. Fc-tagged fusion constructs: cDNA encoding Fc protein was cloned into the pAptag5 vector at N or C termini of hevin fragments or NRX1-ECDs. Recombinant Fc-tagged proteins were purified from HEK293-conditioned media using HiTRAP protein G affinity columns (GE Healthcare).

RGC Transfections

RGCs were transfected using the Lipofectamine LTX (Invitrogen) reagent on DIV5. Hevin treatments started 2 days post-shRNA transfection. The number of synapses on EGFP positive cells was quantified as in Ippolito and Eroglu (2010).

Presynaptic "Hemisynapse" Assay

HA-tagged TM constructs or NL1-expressing HEK293 cells were co-cultured with RGCs (DIV6). Three days later, cells were fixed and stained for synapsin-1 and imaged using a Zeiss 710 inverted confocal microscope.

Postsynaptic "Bead Clustering" Assay

Fc-tagged proteins on protein G-coated magnetic beads were added onto cultured RGCs. After 3 days, RGCs were fixed and stained for homer-1 and Fc. Confocal images of cells were taken at 40 \times magnification for quantification.

NRX-NL Co-clustering Assay

CFP-tagged α or β NRX1-expressing COS7 cells were co-cultured with HA-NL1B-expressing RGCs (DIV6) in the presence or absence of purified hevin or hevin mutants (100 nM each). After 3 days of co-culture, cells were fixed and stained. Confocal images of CFP-expressing COS7 cells were analyzed for clustering of NL1B.

Hevin Injections and Synapse Analyses

Hevin KO (Kucukdereli et al., 2011) and NL1 KO (Varoquaux et al., 2006) mice were previously described. The NRX1 α KOs (Grayton et al., 2013) were received from Catherine Fernandes (King's College London) and crossed into a mixed background.

Hevin or Hevin- Δ DE were injected into the V1 cortices of P13 Hevin KO, and NL1 HET or KO mice and the brains were harvested and analyzed for synapse numbers at P16 using methods described in Risher et al. (2014).

AAV2/5 Preparation and Administration

Full-length hevin cDNA was cloned into the pZac2.1 gfaABC1D-Cyto-GCaMP3 viral vector (Addgene plasmid #44331) replacing the GCaMP3 sequence. Human GFAP promoter (gfaABC1D) is highly selective for astrocytes (Shigetomi et al., 2013). AAV2/5-Hevin (1.82×10^{13} GC/ml) (50–100 nl) virus was injected into layer IV of V1B of Hevin KO mice at P3.

Ocular Dominance Plasticity Recordings

At P23, littermate Hevin WT, HET, KO, or virus-injected Hevin KO mice were anesthetized with isoflurane. Electrodes were implanted at stereotaxic coordinates corresponding to layer 4 of V1B in each cortical hemisphere. At P26, mice were presented with a visual stimulus to each eye independently and

VEPs were recorded. Recordings were made of >100 stimulus presentations/animal, and peak-to-trough measurements of the largest amplitude VEP response from each eye were measured and averaged. After the baseline recordings, mice were anesthetized with isoflurane, and one eyelid was stitched and glued shut. Mice remained monocularly deprived for a period of 7 days and VEP recording procedure was repeated. Contralateral bias indices (CBI) was calculated as the ratio of the contralateral VEP over the ipsilateral VEP response for each mouse.

Statistics

Statistical analyses were performed using Statistica Software. Individual statistical tests can be found in their respective figure legends.

SUPPLEMENTAL INFORMATION

Supplemental Information includes Supplemental Experimental Procedures and seven figures and can be found with this article online at <http://dx.doi.org/10.1016/j.cell.2015.11.034>.

AUTHOR CONTRIBUTIONS

S.K.S., J.A.S., N.P., H.D., Y.H.K., L.-J.P., A.P., S.H.S., D.L.S., R.R.J., A.E.M., and C.E. designed research. S.K.S., J.A.S., N.P., H.D., Y.H.K., L.-J.P., I.H.K., A.C.M., W.S.R.-J., A.P., Z.E., and C.E. performed research. P.S. contributed reagents and data analysis tools. S.K.S., J.A.S., N.P., H.D., Y.H.K., A.P., E.E., A.E.M., and C.E. analyzed data. S.K.S., J.A.S., A.E.M., and C.E. wrote the paper.

ACKNOWLEDGMENTS

We thank Drs. Anne-Marie Craig and Tabreez Siddique for providing Nrx constructs, Dr. Helene Sage for sharing many hevin reagents, and Drs. Anne West and Nicola Allen for critical reading of the manuscript. This research was funded by an NIH/NIDA R01 (DA031833) and Brumley Neonatal Perinatal Research Institute grant to C.E., an NIH/NIDCR R01 (DE22743) to R.R.J., an NIH/NIAAA R01 (AA0130123) to A.E.M., an NIH/NIMH R01 (MH103374) to S.H.S., an R01 NIH/NINDS (NS083897) to D.L.S., and by Swiss National Science Foundation to P.S. S.K.S. and H.D. are Ruth K. Broad International Postdoctoral Fellows. J.A.S. is funded by F31 NIH/NINDS (NS092419). A.P. was funded by an HHMI VIP grant. C.E. is a Holland-Trice Brain Research Scholar, Esther and Joseph Klingenstein Fund Fellow, and Alfred P. Sloan Fellow.

Received: November 21, 2014

Revised: August 18, 2015

Accepted: November 10, 2015

Published: January 14, 2016

REFERENCES

- Baudouin, S., and Scheiffele, P. (2010). SnapShot: neuroligin-neurexin complexes. *Cell* **141**, 908.
- Bear, M.F., Kleinschmidt, A., Gu, Q.A., and Singer, W. (1990). Disruption of experience-dependent synaptic modifications in striate cortex by infusion of an NMDA receptor antagonist. *J. Neurosci.* **10**, 909–925.
- Boucard, A.A., Chubykin, A.A., Comoletti, D., Taylor, P., and Südhof, T.C. (2005). A splice code for trans-synaptic cell adhesion mediated by binding of neuroligin 1 to alpha- and beta-neurexins. *Neuron* **48**, 229–236.
- Bourne, H.R., and Nicoll, R. (1993). Molecular machines integrate coincident synaptic signals. *Cell* **72** (Suppl.), 65–75.
- Budreck, E.C., Kwon, O.B., Jung, J.H., Baudouin, S., Thommen, A., Kim, H.S., Fukazawa, Y., Harada, H., Tabuchi, K., Shigemoto, R., et al. (2013). Neuroligin-1 controls synaptic abundance of NMDA-type glutamate receptors through extracellular coupling. *Proc. Natl. Acad. Sci. USA* **110**, 725–730.
- Chih, B., Engelman, H., and Scheiffele, P. (2005). Control of excitatory and inhibitory synapse formation by neuroligins. *Science* **307**, 1324–1328.
- Chih, B., Gollan, L., and Scheiffele, P. (2006). Alternative splicing controls selective trans-synaptic interactions of the neuroligin-neurexin complex. *Neuron* **51**, 171–178.
- Chubykin, A.A., Atasoy, D., Etherton, M.R., Brose, N., Kavalali, E.T., Gibson, J.R., and Südhof, T.C. (2007). Activity-dependent validation of excitatory versus inhibitory synapses by neuroligin-1 versus neuroligin-2. *Neuron* **54**, 919–931.
- Chung, W.S., Allen, N.J., and Eroglu, C. (2015). Astrocytes control synapse formation, function, and elimination. *Cold Spring Harb. Perspect. Biol.* **7**, a020370.
- Coleman, J.E., Law, K., and Bear, M.F. (2009). Anatomical origins of ocular dominance in mouse primary visual cortex. *Neuroscience* **161**, 561–571.
- Craig, A.M., and Kang, Y. (2007). Neurexin-neuroligin signaling in synapse development. *Curr. Opin. Neurobiol.* **17**, 43–52.
- De Rubeis, S., He, X., Goldberg, A.P., Poultney, C.S., Samocha, K., Cicek, A.E., Kou, Y., Liu, L., Fromer, M., Walker, S., et al.; DDD Study; Homozygosity Mapping Collaborative for Autism; UK10K Consortium (2014). Synaptic, transcriptional and chromatin genes disrupted in autism. *Nature* **515**, 209–215.
- Frenkel, M.Y., and Bear, M.F. (2004). How monocular deprivation shifts ocular dominance in visual cortex of young mice. *Neuron* **44**, 917–923.
- Graf, E.R., Zhang, X., Jin, S.X., Linhoff, M.W., and Craig, A.M. (2004). Neurexins induce differentiation of GABA and glutamate postsynaptic specializations via neuroligins. *Cell* **119**, 1013–1026.
- Grayton, H.M., Missler, M., Collier, D.A., and Fernandes, C. (2013). Altered social behaviours in neurexin 1 α knockout mice resemble core symptoms in neurodevelopmental disorders. *PLoS ONE* **8**, e67114.
- Huang, C.S., Shi, S.H., Ule, J., Ruggiu, M., Barker, L.A., Darnell, R.B., Jan, Y.N., and Jan, L.Y. (2005). Common molecular pathways mediate long-term potentiation of synaptic excitation and slow synaptic inhibition. *Cell* **123**, 105–118.
- Ippolito, D.M., and Eroglu, C. (2010). Quantifying synapses: an immunocytochemistry-based assay to quantify synapse number. *J. Vis. Exp.* **45**, 2270.
- Jacquemont, M.L., Sanlaville, D., Redon, R., Raoul, O., Cormier-Daire, V., Lyonnet, S., Amiel, J., Le Merrer, M., Heron, D., de Blois, M.C., et al. (2006). Array-based comparative genomic hybridisation identifies high frequency of cryptic chromosomal rearrangements in patients with syndromic autism spectrum disorders. *J. Med. Genet.* **43**, 843–849.
- Johnston, I.G., Paladino, T., Gurd, J.W., and Brown, I.R. (1990). Molecular cloning of SC1: a putative brain extracellular matrix glycoprotein showing partial similarity to osteonectin/BM40/SPARC. *Neuron* **4**, 165–176.
- Kahler, A.K., Djurovic, S., Kulle, B., Jonsson, E.G., Agartz, I., Hall, H., Opjordsmoen, S., Jakobsen, K.D., Hansen, T., Melle, I., et al. (2008). Association analysis of schizophrenia on 18 genes involved in neuronal migration: MDGA1 as a new susceptibility gene. *Am. J. Med. Genet. B Neuropsychiatr. Genet.* **147B**, 1089–1100.
- Krahe, T.E., and Medina, A.E. (2010). Activation of NMDA receptors is necessary for the recovery of cortical binocularity. *J. Neurophysiol.* **103**, 2700–2706.
- Kucukdereli, H., Allen, N.J., Lee, A.T., Feng, A., Ozlu, M.I., Conatser, L.M., Chakraborty, C., Workman, G., Weaver, M., Sage, E.H., et al. (2011). Control of excitatory CNS synaptogenesis by astrocyte-secreted proteins Hevin and SPARC. *Proc. Natl. Acad. Sci. USA* **108**, E440–E449.
- Lee, H., Dean, C., and Isacoff, E. (2010). Alternative splicing of neuroligin regulates the rate of presynaptic differentiation. *J. Neurosci.* **30**, 11435–11446.
- Missler, M., Zhang, W., Rohlmann, A., Kattenstroth, G., Hammer, R.E., Gottmann, K., and Südhof, T.C. (2003). Alpha-neurexins couple Ca²⁺ channels to synaptic vesicle exocytosis. *Nature* **423**, 939–948.
- Nair, A., Treiber, J.M., Shukla, D.K., Shih, P., and Muller, R.A. (2013). Impaired thalamocortical connectivity in autism spectrum disorder: a study of functional and anatomical connectivity. *Brain* **136**, 1942–1955.
- Porciatti, V., Pizzorusso, T., and Maffei, L. (1999). The visual physiology of the wild type mouse determined with pattern VEPs. *Vision Res.* **39**, 3071–3081.

- Purcell, A.E., Jeon, O.H., Zimmerman, A.W., Blue, M.E., and Pevsner, J. (2001). Postmortem brain abnormalities of the glutamate neurotransmitter system in autism. *Neurology* 57, 1618–1628.
- Risher, W.C., Patel, S., Kim, I.H., Uezu, A., Bhagat, S., Wilton, D.K., Pilaz, L.J., Singh Alvarado, J., Calhan, O.Y., Silver, D.L., et al. (2014). Astrocytes refine cortical connectivity at dendritic spines. *eLife* 3. <http://dx.doi.org/10.7554/eLife.04047>.
- Roberts, E.B., Meredith, M.A., and Ramoa, A.S. (1998). Suppression of NMDA receptor function using antisense DNA block ocular dominance plasticity while preserving visual responses. *J. Neurophysiol.* 80, 1021–1032.
- Sawtell, N.B., Frenkel, M.Y., Philpot, B.D., Nakazawa, K., Tonegawa, S., and Bear, M.F. (2003). NMDA receptor-dependent ocular dominance plasticity in adult visual cortex. *Neuron* 38, 977–985.
- Scheiffele, P., Fan, J., Choih, J., Fetter, R., and Serafini, T. (2000). Neuroligin expressed in nonneuronal cells triggers presynaptic development in contacting axons. *Cell* 101, 657–669.
- Schreiner, D., Simicevic, J., Ahn , E., Schmidt, A., and Scheiffele, P. (2015). Quantitative isoform-profiling of highly diversified recognition molecules. *eLife* 4, e07794.
- Shigetomi, E., Bushong, E.A., Hausteine, M.D., Tong, X., Jackson-Weaver, O., Kracun, S., Xu, J., Sofroniew, M.V., Ellisman, M.H., and Khakh, B.S. (2013). Imaging calcium microdomains within entire astrocyte territories and endfeet with GCaMPs expressed using adeno-associated viruses. *J. Gen. Physiol.* 141, 633–647.
- Siddiqui, T.J., Pancaroglu, R., Kang, Y., Rooyakkers, A., and Craig, A.M. (2010). LRRTMs and neuroligins bind neurexins with a differential code to cooperate in glutamate synapse development. *J. Neurosci.* 30, 7495–7506.
- Smith, S.L., and Trachtenberg, J.T. (2007). Experience-dependent binocular competition in the visual cortex begins at eye opening. *Nat. Neurosci.* 10, 370–375.
- S dhof, T.C. (2008). Neuroligins and neurexins link synaptic function to cognitive disease. *Nature* 455, 903–911.
- Tropea, D., Kreiman, G., Lyckman, A., Mukherjee, S., Yu, H., Hornig, S., and Sur, M. (2006). Gene expression changes and molecular pathways mediating activity-dependent plasticity in visual cortex. *Nat. Neurosci.* 9, 660–668.
- Varoqueaux, F., Aramuni, G., Rawson, R.L., Mohrmann, R., Missler, M., Gottmann, K., Zhang, W., S dhof, T.C., and Brose, N. (2006). Neuroligins determine synapse maturation and function. *Neuron* 51, 741–754.
- Vialou, V., Robison, A.J., Laplant, Q.C., Covington, H.E., 3rd, Dietz, D.M., Ohnishi, Y.N., Mouzon, E., Rush, A.J., 3rd, Watts, E.L., Wallace, D.L., et al. (2010). DeltaFosB in brain reward circuits mediates resilience to stress and antidepressant responses. *Nat. Neurosci.* 13, 745–752.
- Weaver, M.S., Workman, G., Cardo-Vila, M., Arap, W., Pasqualini, R., and Sage, E.H. (2010). Processing of the matricellular protein hevin in mouse brain is dependent on ADAMTS4. *J. Biol. Chem.* 285, 5868–5877.
- Zhurov, V., Stead, J.D., Merali, Z., Palkovits, M., Faludi, G., Schild-Poulter, C., Anisman, H., and Poulter, M.O. (2012). Molecular pathway reconstruction and analysis of disturbed gene expression in depressed individuals who died by suicide. *PLoS ONE* 7, e47581.